Molecular cloning and immunolocalization of a novel vertebrate *trp* homologue from *Xenopus*

Laura K. BOBANOVIĆ*[1], Mika LAINE*[1], Carl C. H. PETERSEN*[1,2], Deborah L. BENNETT*[1,3], Michael J. BERRIDGE*†, Peter LIPP*[4], Scott J. RIPLEY* and Martin D. BOOTMAN*†

*Laboratory of Molecular Signalling, The Babraham Institute, Babraham, Cambridge CB2 4AT, U.K., and †Department of Zoology, University of Cambridge, Downing Street, Cambridge CB2 3EJ, U.K.

We report the sequence, structure and distribution of a novel transient receptor potential (*trp*) homologue from *Xenopus*, *Xtrp*, determined by screening an oocyte cDNA library. On the basis of sequence similarity and predicted structure, *Xtrp* appears to be a homologue of mammalian *trp1* proteins. Two polyclonal antibodies raised against distinct regions of the *Xtrp* sequence revealed *Xtrp* expression in various *Xenopus* tissues, and the localization of *Xtrp* at the plasma membrane of *Xenopus* oocytes and HeLa cells. Since capacitative calcium entry into *Xenopus* oocytes has been shown previously to be substantially inhibited by *trp1* antisense oligonucleotides [Tomita, Kaneko, Funayama, Kondo, Satoh and Akaike (1998) Neurosci. Lett. **248**, 195–198] we suggest that *Xtrp* may underlie capacitative calcium entry in *Xenopus* tissues.

INTRODUCTION

In both non-excitable and excitable cells, a mechanism of agonist-induced calcium signalling depends upon the activation of phospholipase C to increase the intracellular level of Ins(1,4,5)P_3. Binding of Ins(1,4,5)P_3 to specific receptors allows calcium to exit from intracellular Ins(1,4,5)P_3-sensitive calcium stores, causing a rapid increase in the intracellular calcium concentration [1]. Prolonged responses to agonist-induced calcium signalling are maintained by the opening of calcium-permeable plasma membrane channels that enable calcium to enter from the extracellular space. This entry is coupled to store depletion through a 'capacitative calcium entry' (CCE) mechanism that remains speculative and controversial [2,3].

One approach to identify the mechanism underlying activation of CCE is to characterize the store-operated channels (SOCs) responsible for the calcium current. The transient receptor potential (*trp*) protein of *Drosophila* and its mammalian homologues have been suggested to form these SOCs [4]. Molecular cloning of the *Drosophila trp* (*Dtrp*) protein [5] and the related *trp*-like protein (*Dtrpl*) [6] revealed structural similarities to voltage- and second-messenger-operated ion channels [7].

The possibility that *trp* channels may function as SOCs is supported by the observation that the expression of *Dtrp* in Sf9 insect cells induced a novel calcium-selective current upon depletion of intracellular calcium stores by thapsigargin [8]. Similarly, the amplitude of the calcium-activated chloride currents driven by SOCs in *Xenopus* oocytes was augmented by the expression of *Dtrp* [9]. Additional support for *trp* encoding SOCs came from experiments where endogenous store-operated calcium influx was inhibited by antisense oligonucleotides directed against all six non-allelic *trp* genes [10].

Recent molecular characterization has revealed the existence of multiple genes encoding mammalian *trp* homologues in cells from various organisms [9–22]. Although expression studies have suggested that at least some of the mammalian *trp* homologues may function as SOCs, the hypothesis is still controversial [13,14,16,21,23–25].

The existence of numerous isoforms and the possibility that channels may be composed of different *trp* subunits [26], highlights the difficulty of trying to establish which isoforms may function in CCE. Recently, the expression of five mammalian *trp* homologues (*trp1*, *trp3*–*trp6*) was determined in different tissues and cell lines, three of which were known to exhibit specific calcium-release-activated calcium channels responsible for CCE. It was shown that Jurkat and RBL cells have remarkably similar calcium-release-activated calcium current, even though they express different *trp* isoforms, suggesting that more than one *trp* isoform may participate in CCE [27]. This has been confirmed by expression studies in which both *trp1* and *trp4* have been implicated in CCE, with the most pronounced activity associated with *trp4* [13,14]. Furthermore, it has been proposed that heteromultimer formation by multiple *trp* isoforms may be necessary to elicit native CCE [26,28], although the actual arrangement is unknown.

Xenopus oocytes have been a widely used model for CCE studies [29–31], and have been shown to exhibit enhanced CCE when *trp* proteins are heterologously introduced [9,32]. However, the identity of the endogenous oocyte CCE channels is unknown. In the present study, we report the full-length cloning of a novel *trp* homologue, *Xtrp*, from *Xenopus laevis*. The encoded protein is most similar to mammalian *trp1* proteins. In a recent study, it was found that antisense oligonucleotides directed against the human *trp1* protein could inhibit the endogenous CCE in *Xenopus* oocytes [32]. Based on sequence similarity, the target for the antisense oligonucleotide was most likely the *Xtrp* protein described in the present study. We therefore suggest that *Xtrp* underlies CCE in *Xenopus* oocytes. Antibodies raised against

Abbreviations used: CCE, capacitative calcium entry; SOC, store-operated channel; *trp*, transient receptor potential; *Htrp*, *Btrp*, *Rtrp*, *Mtrp* and *Dtrp*, human, bovine, rat, mouse and *Drosophila trp* proteins respectively.

[1] These authors contributed equally to this work.

[2] Present address: Max-Planck-Institut für medizinisches Forschung, Abteilung Zellphysiologie, 69120 Heidelberg, Germany.

[3] Present address: Department of Veterinary Preclinical Sciences, University of Liverpool, P.O. Box 147, Liverpool L69 3BX, U.K.

[4] To whom correspondence should be addressed (e-mail peter.lipp@bbsrc.ac.uk).

The *Xtrp* nucleotide sequence reported in this paper has been submitted to the GenBank/EBI Data Bank with accession number AF113508.

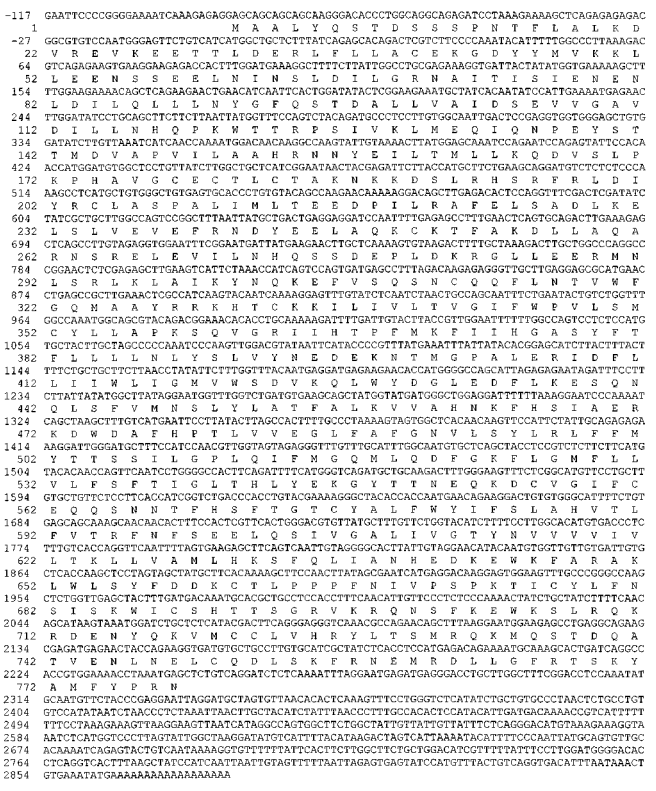

Figure 1 Nucleotide sequence of *Xtrp* cDNA and amino acid sequence alignment of *Xtrp* with mammalian *trp1* homologues

Xtrp nucleotide and amino acid sequence. The numbers of amino acids and nucleotides are given on the left. Amino acids are numbered starting from the first methionine residue.

Xtrp indicate that it is expressed in various *Xenopus* tissues, particularly in excitable cells. Furthermore, immunostaining of *Xenopus* oocytes indicated the expression of *Xtrp* solely in the plasma membrane.

EXPERIMENTAL

Preparation of cells and tissues

Oocytes were obtained from *X. laevis* according to a procedure described previously [33]. Fully grown stage VI oocytes (1.2–1.3 mm diam.) were manually defolliculated. Oocytes and tissues dissected from *X. laevis* were rinsed and disrupted in homogenization buffer [50 mM Tris/HCl, pH 8.3/1 mM EDTA containing protease inhibitors C*θ*mplete™, Mini (Boehringer Mannheim)]. The resulting homogenate was centrifuged at 500 ***g*** at 4 °C for 5 min, and the supernatant was centrifuged at 25000 ***g*** for 15 min at 4 °C to pellet the microsomal fraction. The pellet was resuspended at 5–10 mg/ml in homogenization buffer.

Isolation of a *Xenopus* trp cDNA

A *Xenopus* oocyte cDNA library in pBluescript RN3 [kindly provided by Professor J. Gurdon (Wellcome C. R. C., Cambridge, U.K.)] was plated and screened using a ^{32}P-labelled 304 bp PCR product cloned previously from *Xenopus* oocyte cDNA as a probe [9]. Hybridizing colonies were purified by successive rounds of screening. Two positive clones were obtained and the one containing the largest insert was subjected to DNA sequencing.

DNA sequencing and sequence analysis

Overlapping deletions were generated by exonuclease III digestion (Exo Mung Bean Deletion Kit; Stratagene) in accordance with the manufacturer's protocol. The cDNAs were sequenced in both directions by the Sanger dideoxy-mediated chain-termination method [34], using Sequenase Version 2.0 (Amersham). The sequence was assembled with the Genetics Computer Group Sequence Analysis Software package and new sequencing primers designed to complete any missing sequence. Database searches, sequence alignments and analysis were also performed using Genetics Computer Group software.

Preparation of antibodies

Synthetic peptides, EL-1, based on the sequence of amino acid residues 557–575 (V-G-I-F-C-E-Q-Q-S-N-N-T-F-H-S-F-T-G-T), and CT-1, based on the amino acid residues 703–720 (K-E-W-K-S-L-R-Q-K-R-D-E-N-Y-Q-K-V-M) of the *Xtrp* were synthesized using the standard Fmoc (fluoren-9-ylmethoxycarbonyl) method on the Perceptive Biosystems synthesizer (Microchemical Facility, Babraham Institute, Cambridge, U.K.). The sequence of EL-1, corresponding to a putative extracellular loop between segments 5 and 6 of *Xtrp*, and the sequence of CT-1, corresponding to the intracellular region following the sixth transmembrane segment on the C-terminus (see Figure 2 and Figure 3) were synthesized with additional cysteine residues at the N- and C-termini to facilitate coupling reactions. The peptides were coupled to the purified protein derivative of tuberculin and initially rabbits were injected intramuscularly with 1 mg of antigen followed by a booster injection of 500 μg at intervals of 3 weeks. Crude antiserum was collected 10 days after each boost.

Five different polyclonal antibodies to the *Xtrp* sequence were generated, and the EL-1 and CT-1 antisera used in the present study were the most reliable. The specificity of each antiserum was tested using several different approaches. First, immunoblotting confirmed that they all specifically recognized the peptide sequences against which they were raised. Secondly, in Western blots, the antisera intensely stained single bands of the expected molecular mass. Finally, Western blots of *Xtrp*–GFP fusion proteins were performed and it was found that anti-*Xtrp* antibodies recognized the same band as anti-GFP antibodies. From these observations we suggest that the antibodies were highly specific for *Xtrp*.

Purification of the antisera

A large-scale purification of the antisera was accomplished using affinity chromatography as described previously [35]. Briefly, 3 ml of the crude antiserum was applied to 1 mg of the peptide covalently bound to 2 ml of solid gel (Sulfolink matrix; Pierce and Wariner, Chester, U.K.) and recirculated overnight at 4 °C through the resin placed in the glass column. After washing with 0.1 M PBS, the antibodies were eluted with 100 mM glycine (pH 2.5) and neutralized with 1 M Tris/HCl (pH 8.0). The dialysate was concentrated using a Minicon B-15 concentrator (Amicon) and resuspended in storage buffer [0.1 PBS/0.2 % (w/v) BSA].

Immunoblot analysis

Proteins were analysed by SDS/PAGE (6 % gel) according to the method of Laemmli [36]. The polypeptides separated in the gels were transferred on to 0.45-μm PVDF membranes (Immobilon-

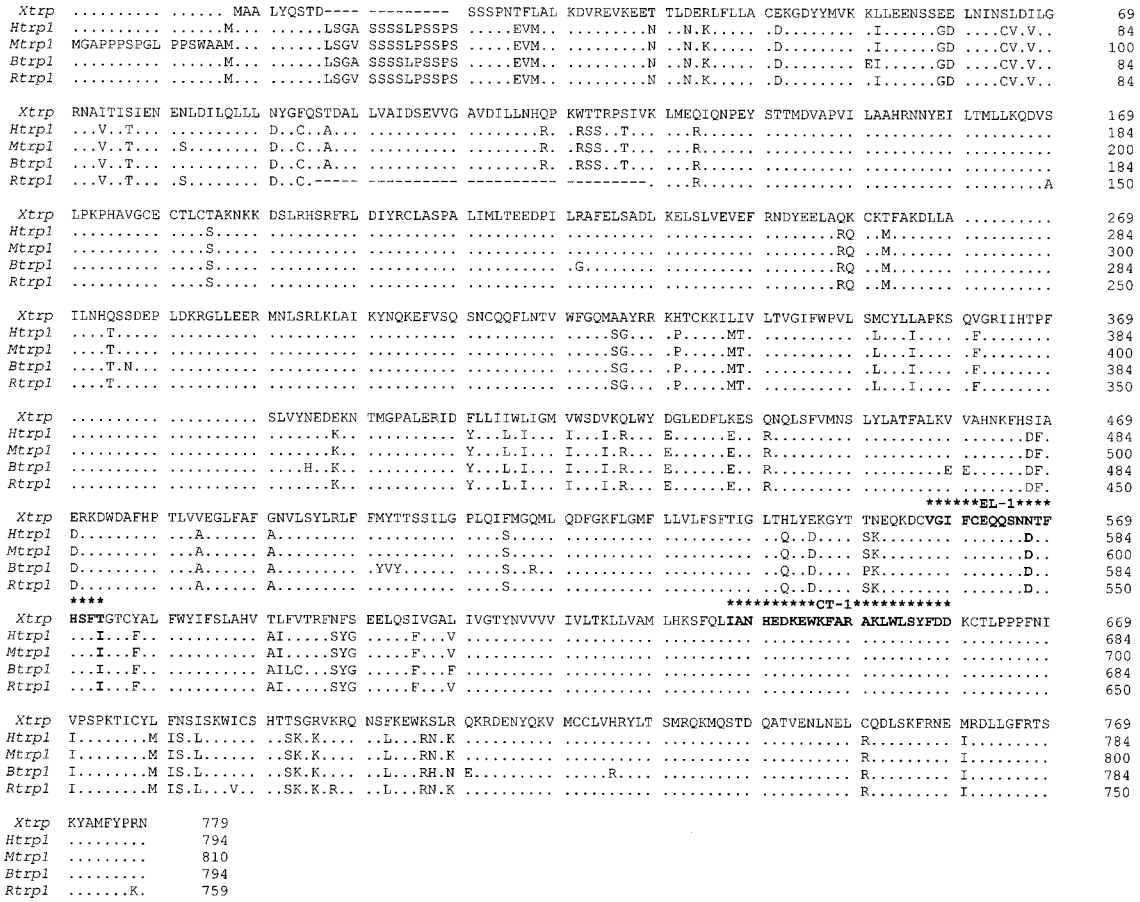

Figure 2 Amino acid sequence alignment of *trp1* homologues

Xtrp was aligned to the published full-length sequences of *Htrp1* [12], *Mtrp1* [17], *Btrp1* [18] and *Rtrp1* (GenBank accession number AF061266) using MultiAlign [40]. Numbers of amino acids are given at the right. Identical residues with respect to *Xtrp* are represented by a dot (.). Dashes (—) indicate a gap. The location of peptide sequences used to raise antisera EL-1 and CT-1 are indicated in bold type and with asterisks.

P; Millipore) at 90 mA constant current for 2 h. PVDF membranes were blocked for non-specific binding with 5% (w/v) skimmed milk (Marvel) in PBS/0.1% (v/v) Tween 20 (PBS-T) overnight at 4 °C, and this was followed by incubation with the primary antibodies (EL-1 or CT-1 at 1:1000 dilution) in PBS-T with 2% (w/v) BSA for 2 h. The membrane was washed a further three times (5 min per wash) in PBS-T and then incubated for 1 h at room temperature in 5% (w/v) skimmed milk in PBS-T with the secondary antibody (horseradish peroxidase conjugated with anti-rabbit IgG at 1:2000 dilution; Vector Laboratories). The membranes were then washed three times for 5 min in PBS-T and visualized with enhanced chemiluminescence reagent in accordance with manufacturers' instructions (NEN™; Life Science Products). Bound antibody was detected using the Renaissance enhanced chemiluminescence system and Kodak X-OMAT film.

Immunocytochemistry

Freshly isolated *Xenopus* oocytes were defoliculated and fixed for 4 h in methanol at −20 °C [37]. To cryoprotect oocytes before freezing, the fixative was replaced with 30% (w/v) sucrose in PBS (pH 7.4) at 4 °C overnight. Oocytes embedded in O.C.T. Compound (BDH) were frozen on solid CO_2, and sections were cut using a Bright Microtome 5030 (Bright Instrument Company). Slices 26-μm thick were mounted on electrostatically charged microscope slides (Superfrost Plus Microscope Slides; BDH) and left to dry in air.

For indirect immunocytochemistry, sections were incubated for 2 h in PBS/2% (w/v) BSA to block the non-specific binding, and incubated overnight at 4 °C with *Xtrp* antibodies (EL-1 and CT-1). After three washings of 10 min each in PBS, sections were incubated in PBS which contained fluorescein-labelled anti-rabbit IgG secondary antibody (1:200; Vector Laboratories) and 2% (w/v) BSA for 2 h at room temperature. Finally, after three washes of 10 min with PBS, stained sections were mounted using Vectashield mounting medium (Vector Laboratories) and left to dry in the dark. In control experiments, the incubation steps with primary antibodies were omitted. Immunohistochemical stainings were visualized using an UltraVIEW confocal microscope (Life Science Resources, Cambridge, U.K.) using ×60, ×20 and ×4 objectives (Olympus).

RESULTS

Using a PCR-based strategy with degenerate oligonucleotides derived from mouse brain *trp*, we previously demonstrated the existence of a vertebrate *trp* homologue in *Xenopus* oocytes [9].

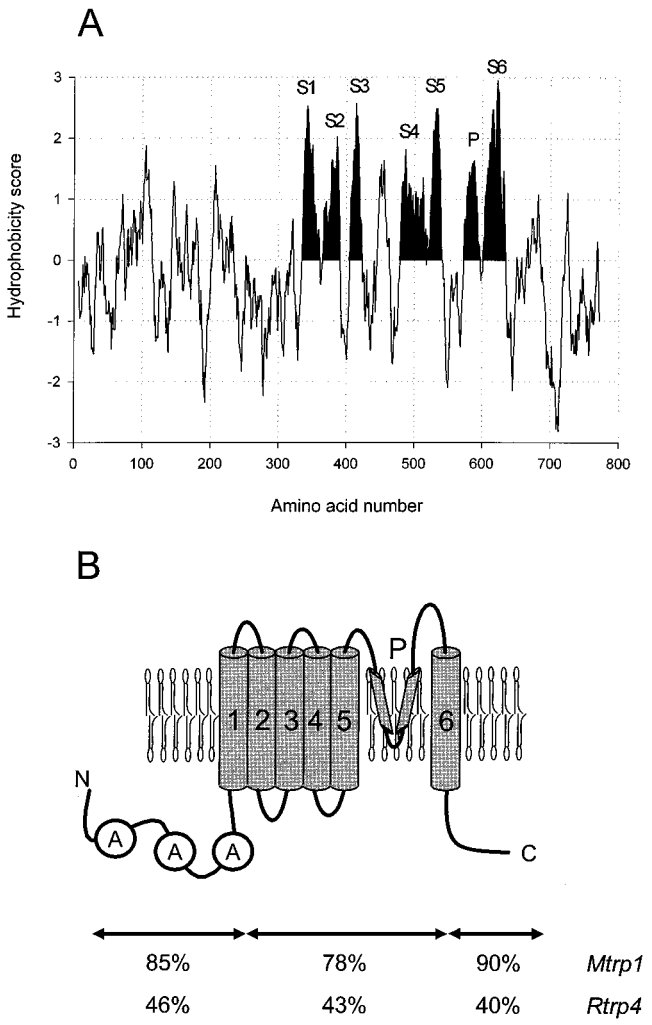

Figure 3 Structural characteristics of *Xtrp*

(**A**) Hydrophobicity plot of *Xtrp* obtained according to the Kyte–Doolittle method [41] using a window size of 13 amino acids. The putative transmembrane segments (S1–S6) and the putative pore loop (P) are shown. (**B**) Putative domain structure and topology of *Xtrp* represented as N-terminal, transmembrane and C-terminal domains. The degree of amino acid identity between *Xtrp* and the three major domains within mammalian *Mtrp1* and *Rtrp4* is shown for each domain at the bottom of the Figure. The putative transmembrane segments (1–6), the putative pore loop (P) and ankyrin-like domains (A) are depicted.

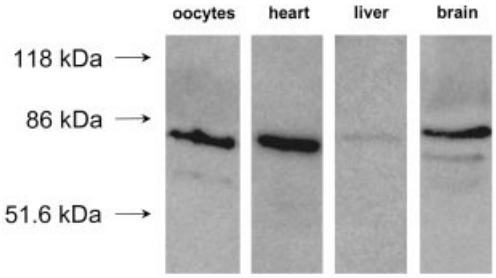

Figure 4 Western-blot analysis of *Xtrp* protein in *Xenopus* oocytes and *Xenopus* tissues

Microsomal preparations from oocytes (100 μg of protein), heart, liver and brain (each 30 μg of protein) were subjected to SDS/PAGE (see the Experimental section). The subsequent immunoblots were probed with CT-1 antisera at dilution 1:1000. The data shown are representative of three analyses of two independent tissue preparations.

To allow comparison with other *trp*s, we sought to obtain a full-length *Xtrp* cDNA using library screening (see the Experimental section). The 2998 nt sequence of the cloned *Xtrp* cDNA contained a single open reading frame of 2334 bp encoding a protein of 778 amino acids (Figure 1) with a molecular mass of 90 kDa.

Sequence alignment of *Xtrp* with known full-length mammalian *trp* sequences show that this newly-isolated vertebrate *trp* protein most closely resembled *trp1* isoforms (Figure 2). The amino acid sequence of *Xtrp* was 82% identical (88% similar) with mouse *trp1* (*Mtrp*1) and human *trp1* (*Htrp1*), 81% identical (87% similar) with bovine *trp1* (*Btrp1*) and 78% identical (84% similar) with rat *trp1* (*Rtrp1*). When compared with other mammalian *trp* isoforms, the identities were much lower, the highest was 44% for rat *trp4* (results not shown). At the nucleotide level, *Xtrp* was 78% identical with *Mtrp1*, 77% identical with *Htrp1* and 76% identical with *Btrp1*. The degree of amino acid sequence identity varied considerably within the different structural domains. A putative cytoplasmic region in the C-terminal domain (residues 631–778) was most conserved with 90% of residues being identical with mammalian *trp1* family members. The identity between *Xtrp* and mammalian *trp1* in the putative transmembrane segment (residues 336–630) was 78%. Finally, the N-terminal domain (residues 1–335) was 85% identical with the N-termini of the mammalian *trp1* proteins.

Hydrophobicity analysis indicated the presence of eight hydrophobic regions, and hydrophilic N- and C-termini (Figure 3), similar to that predicted for other *trp* homologues [5,10–12,14–16,20,21]. It is likely that not all eight of the hydrophobic regions were membrane spanning, since the third and seventh putative regions were not sufficiently hydrophobic. Therefore, in accordance with the model proposed by Birnbaumer et al. [26], and by analogy to voltage-operated channels, *Xtrp* is likely to be a six-transmembrane spanning protein (segments S1–S6 in Figure 3A), with a putative pore region (P in Figures 3A and 3B). Long cytoplasmic domains at the N- and C-termini flanked the hydrophobic core that makes up the channel. The N-terminal region also contained three ankyrin-like motifs (denoted 'A' in Figure 3B).

Antipeptide antibodies generated against two regions of the *Xtrp* sequence (regions marked with bold type in Figure 2), were used for Western blot analysis of *Xenopus* brain, liver, heart and oocyte preparations. Intensely staining bands, with an approx. molecular mass of 80 kDa, were observed in heart and brain tissue with both EL-1 and CT-1 antibodies. A lower level of staining was observed in oocytes and a much fainter band was detected in liver (Figure 4). Both EL-1 and CT-1 antisera recognized the same 80 kDa protein in *Xenopus* protein preparations. The protein detected by EL-1 and CT-1 was $\sim$ 10 kDa smaller than the predicted mass for the *Xtrp* based upon sequence data (see above). However, a similar observation was reported for the expression of *trpC1* in Sf9 cells, where recombinant FLAG–*TrpC1* also ran at a lower molecular mass than expected upon SDS/PAGE [25], possibly due to post-translation processing.

To determine the sub-cellular localization of *Xtrp*, immunocytochemistry was performed on *Xenopus* oocyte sections. Sections stained with both CT-1 and EL-1 antibodies displayed intense immunofluorescence at the plasma membrane (Figures 5A–5F). No significant staining above background was seen in the rest of the cell, except for a faint signal around the nuclear membrane (Figure 5A), which was also detectable in controls

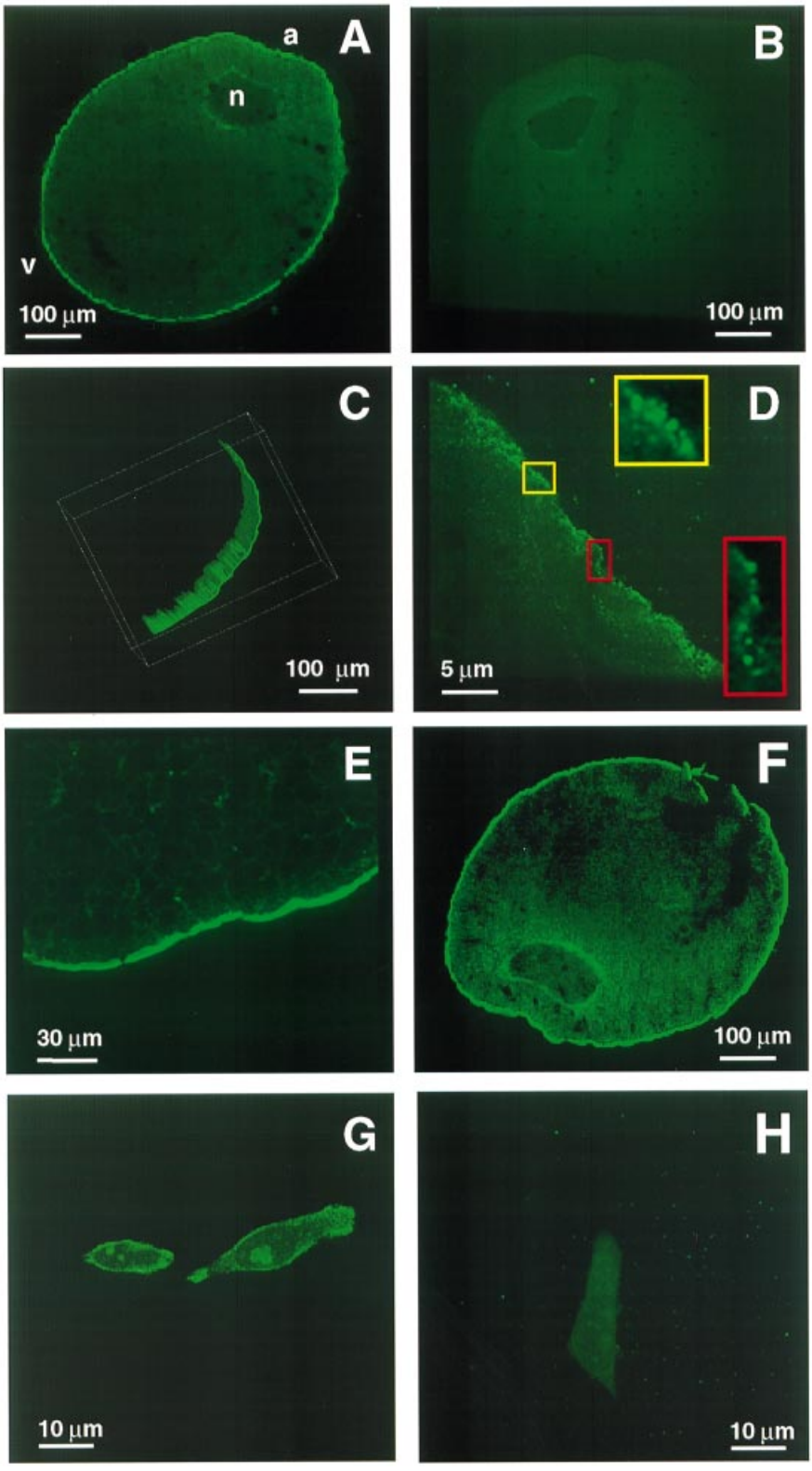

Figure 5 Immunofluorescent staining of *Xtrp* protein in *Xenopus* oocyte cryosections and HeLa cells

(**A**) Immunofluorescent labelling of an oocyte using CT-1 antibody (1:25 dilution). The animal (a) and vegetal (v) poles and the nucleus (n) are indicated. (**B**) Control oocyte stained in the absence of primary antibody. (**C**) Partial three-dimensional reconstruction of immunofluorescence from a CT-1-stained oocyte membrane (1:50 dilution) (image rendered using VolumeWIZARD software; Life Science Resources). (**D**) Higher magnification of CT-1 immunofluorescence. The areas of membrane bounded by the boxes have been expanded 5-fold to show the punctate distribution of CT-1 staining. (**E**) and (**F**) Examples of immunofluorescent labelling of *Xenopus* sections using the EL-1 antibody (1:25 dilution). A similar, although more diffuse, immunofluorescence was detected in CT-1-stained HeLa cells (**G**) (1:200 antibody dilution). (**H**) Background staining of HeLa cells (secondary antibody only).

(Figure 5B). At low magnification, a consistent staining was observed all over the plasma membrane, as illustrated in the volume-rendered image in Figure 5(C). At higher magnifications, and using a greater dilution of the antibodies, the plasma membrane staining could be deconvolved into an irregular spot-like pattern (Figure 5D), consistent with a punctate localization of *Xtrp*. The intensity of immunofluorescence showed no significant difference between the animal and vegetal poles of the oocytes (Figure 5A). Comparable staining was obtained using CT-1 (Figures 5A–5D) and EL-1 (Figures 5E and 5F) antibodies.

Based on sequence similarities, the CT-1 and EL-1 antibodies should be specific for *trp1* homologues. This was supported by Western-blot analysis of various mammalian tissues, including HeLa cells and rat atrial and ventricular myocytes, which revealed that these antibodies identified single protein bands (results not shown). Furthermore, immunocytochemical staining of HeLa cells using the CT-1 antibody demonstrated immunoreactivity localized to the plasma membrane (Figure 5G, cf. Figure 5H), similar to that seen in *Xenopus* oocytes. However, the pattern of immunoreactivity in HeLa cells was more diffuse than in *Xenopus* oocytes, with some staining also detectable inside the cells (Figure 5G).

DISCUSSION

In the present study, we describe the full-length cloning, molecular characterization and cellular distribution of a novel *trp* protein, *Xtrp*, from *Xenopus*. This protein has essentially the same structure as mammalian *trp* homologues, with a hydrophobic core and at least six putative transmembrane segments flanked by cytosolic N- and C-terminal domains (Figures 1–3). *Xtrp* is most likely a homologue of the mammalian *trp1* proteins, since sequence comparison reveals significant similarities to *Htrp1* [12], *Mtrp1* [17] and *Btrp1* [18] (Figure 2).

In a recent study of calcium entry in *Xenopus* oocytes, the endogenous CCE current was inhibited in a concentration-dependent manner by antisense oligonucleotides directed against *trp1* proteins [32]. The antisense oligonucleotide used in the study of Tomita et al. [32] was designed using known mammalian *trp1* sequences. On the basis of the nucleotide sequence of *Xtrp* (Figure 1), it is likely that the target of the antisense was the *Xtrp* protein described in this study (70% sequence identity at nt 110–140 of the *Xtrp* sequence). The fact that the antisense oligonucleotide used by Tomita et al. [32] did not exactly match the *Xtrp* sequence may account for the incomplete inhibition of CCE in their study.

It appears, therefore, that *Xtrp* may function as an SOC in *Xenopus* oocytes. In support of this, we found that *Xtrp* was exclusively localized at the plasma membrane in *Xenopus* oocytes (Figure 5). The punctate expression pattern of *Xtrp* was surprising, and suggests that the protein exists in discrete clusters at the plasma membrane. Interestingly, no significant differences in *Xtrp* expression were observed between the vegetal and animal hemispheres of the oocytes. These observations are remarkable, since it is known that the endoplasmatic reticulum and phosphatidylinositol second-messenger system is more abundant in the animal pole [38,39].

One puzzling feature of *trp* proteins is that they appear to be more abundant in excitable tissues than in non-excitable cells. To date, such observations have been made using Northern-blot analysis (e.g. [11,12]). However, our Western-blot analysis of *Xenopus* tissues also confirms this result at the protein level (Figure 4). The relatively low expression of *trp* proteins in non-excitable tissues such as hepatocytes (Figure 4) [27] is paradoxical since these cells have a pronounced CCE mechanism.

The role of *trp* in store-regulated calcium entry is controversial. Experiments using antisense oligonucleotides or heterologous expression, to diminish or enhance *trp* expression respectively, have so far provided the most significant evidence for *trp* homologues forming SOCs. In the present study, we demonstrated that *Xenopus* oocytes, which have been widely used as a model for CCE, also express a *trp* homologue. The localization of *Xtrp* to the plasma membrane, and the fact that it was the likely target for a CCE-inhibiting antisense oligonucleotide [32], support the idea that *Xtrp* plays a role in calcium entry in *Xenopus* oocytes.

We thank Dr David Sattelle and Dr Nigel Mongan for providing *Xenopus* oocytes and Dr Howard Baylis for advice in the cloning procedure. L.K.B. was supported by a Thadeuss Mann Trinity Hall Research Fellowship. M.L. is supported by the Academy of Finland and the Finnish Foundation of Cardiovascular Research. C.C.H.P. was supported by The Wellcome Trust and Trinity College Cambridge. S.J.R was supported by a European Union Grant. M.D.B. is a Royal Society University Research Fellow. This work was supported by the Biotechnology and Biological Sciences Research Council, and by a grant from the European Commission BIOMED2 (BMH4-CT96-0656).

REFERENCES

1 Berridge, M. J. (1993) Nature (London) **361**, 315–325
2 Berridge, M. J. (1995) Biochem. J. **312**, 1–11
3 Putney, J. W. (1997) Cell Calcium **21**, 257–261
4 Hardie, R. C. and Minke, B. (1993) Trends Neurosci. **16**, 371–376
5 Montell, C. and Rubin, G. M. (1989) Neuron **2**, 1313–1323
6 Phillips, A. M., Bull, A. and Kelly, L. E. (1992) Neuroreport **8**, 631–642
7 Jan, L. Y. and Jan, Y. N. (1992) Cell **69**, 715–718
8 Vaca, L., Sinkins, W. G., Hu, Y., Kunze, D. L. and Schilling, W. P. (1994) Am. J. Physiol. **267**, C1501–C1505
9 Petersen, C. C. H., Berridge, M. J., Borgese, M. F. and Bennett, D. L. (1995) Biochem. J. **311**, 41–44
10 Zhu, X., Jiang, M., Peyton, M., Boulay, G., Hurst, R., Stefani, E. and Birnbaumer, L. (1996) Cell **85**, 661–671
11 Wes, P. D., Chevesich, J., Jeromin, A., Rosenberg, C., Stetten, G. and Montell, C. (1995) Proc. Natl. Acad. Sci. U.S.A. **92**, 9652–9656
12 Zhu, X., Chu, P. B., Peyton, M. and Birnbaumer, L. (1995) FEBS Lett. **373**, 193–198
13 Zitt, C., Zobel, A., Obukhov, A. G., Harteneck, C., Kalkbrenner, F., Lückhoff, A. and Schultz, G. (1996) Neuron **16**, 1189–1196
14 Philipp, S., Cavalié, A., Freichel, M., Wissenbach, U., Zimmer, S., Trost, C., Marquart, A., Murakami, M. and Flockerzi, V. (1996) EMBO J. **15**, 6166–6171
15 Funayama, M., Goto, K. and Kondo, H. (1996) Mol. Brain Res. **43**, 259–266
16 Boulay, G., Zhu, X., Peyton, M., Jiang, M., Hurst, R., Stefani, E. and Birnbaumer, L. (1997) J. Biol. Chem. **272**, 29672–29680
17 Sakura, H. and Ashcroft, F. M. (1997) Diabetologia **40**, 528–532
18 Chang, A. S., Chang, S. M., Garcia, R. L. and Schilling, W. P. (1997) FEBS Lett. **415**, 335–340
19 Preuss, K.-D., Nöller, J. K., Krause, E., Göbel, A. and Schulz, I. (1997) Biochem. Biophys. Res. Commun. **240**, 167–172
20 Mori, Y., Takada, N., Okada, T., Wakamori, M., Imoto, K., Wanifuchi, H., Oka, H., Oba, A., Ikenaka, K. and Kurosaki, T. (1998) Neuroreport **9**, 507–515
21 Okada, T., Shimizu, S., Wakamori, M., Maeda, A., Kurosaki, T., Takada, N., Imoto, K. and Mori, Y. (1998) J. Biol. Chem. **273**, 10279–10287
22 Philipp, S., Hambrecht, J., Braslavski, L., Freichel, M., Murakami, M., Cavalié, A. and Flockerzi, V. (1998) EMBO J. **17**, 4274–4282
23 Zitt, C., Obukhov, A. G., Strübing, C., Zobel, A., Kalkbrenner, F., Lückhoff, A. and Schultz, G. (1997) J. Cell. Biol. **138**, 1333–1341
24 Zhu, X., Jiang, M. and Birnbaumer, L. (1998) J. Biol. Chem. **273**, 133–142
25 Sinkins, W. G., Estacion, M. and Schilling, W. P. (1998) Biochem. J. **331**, 331–339
26 Birnbaumer, L., Zhu, X., Jiang, M., Boulay, G., Peyton, M., Vannier, B., Brown, D., Platano, D., Sadeghi, H., Stefani, E. and Birnbaumer, M. (1996) Proc. Natl. Acad. Sci. U.S.A. **93**, 15195–15202
27 Garcia, R. L. and Shilling, W. P. (1997) Biochem. Biophys. Res. Commun. **239**, 279–283
28 Xu, X.-Z. S., Li, H.-S., Guggino, W. B. and Montell, C. (1997) Cell **89**, 1155–1164
29 Parekh, A. B., Terlau, H. and Stuehmer, W. (1993) Nature (London) **364**, 814–818
30 Petersen, C. C. H. and Berridge, M. J. (1994) J. Biol. Chem. **26**, 32246–32253
31 Petersen, C. C. H. and Berridge, M. J. (1995) Biochem. J. **30**, 663–668

32 Tomita, Y., Kaneko, S., Funayama, M., Kondo, H., Satoh, M. and Akaike, A. (1998) Neurosci. Lett. **248**, 195–198
33 Verjans, B., Petersen, C. C. H. and Berridge, M. J. (1994) Biochem. J. **304**, 679–682
34 Sanger, F., Nicklen, S. and Coulson, A. R. (1977) Proc. Natl. Acad. Sci. U.S.A. **74**, 5463–5469
35 Phillips, T., Makoff, A., Brown, S., Rees, S. and Emson, P. (1997) Neuroreport **8**, 3349–3354
36 Laemmli, U. K. (1970) Nature (London) **227**, 680–685
37 Stevens, E. B., Woodward, R., Ho, I. H. M. and Murrell-Lagnado, R. (1997) J. Physiol. **503**, 547–562
38 Berridge, M. J. (1988) J. Physiol. **403**, 589–599
39 Callamaras, N., Sun, X. P., Ivorra, I. and Parker, I. (1998) J. Physiol. **511**, 395–405
40 Corpet, F. (1988) Nucleic Acids Res. **16**, 10881–10890
41 Kyte, J. and Doolittle, R. F. (1982) J. Mol. Biol. **157**, 105–132

Received 12 January 1999/4 March 1999; accepted 29 March 1999